34

MCR-96-1303, Issue 01

Contract Number: NAS8-40633

Membrane Transfer Phenomena (MTP)

Semi-Annual Technical Progress Report

for Period Ending 28 April 1996

Program Manager, Larry Mason

Prepared By:
Lockheed Martin Astronautics Company
Flight Systems Division
P.O. Box 179

Prepare For:
National Aeronautics and Space Administration
George C. Marshall Space Flight Center
Marshall Space Flight Center, AL 35812

Membrane Transport Phenomena (MTP)
Technical Progress Report

This report details the progress of the Membrane Transport Phenomena (MTP) contract NAS8-40633 for the period from November 1995 through April 1996. Progress has been made in several areas of the definition, design, and development of the Membrane Transport Apparatus (MTA) instrument and associated sensors and systems. Progress is also reported in the development of software modules for instrument control, experimental image and data acquisition, and data analysis. All of the work reported here was performed by the Principal Investigator, Larry Mason.

The initial MTA instrument development effort is substantially complete, and critical assemblies of the instrument have been defined. The volumetric flow sensors and optical refractometer system have been characterized, and a first osmosis experiment has been performed. The preliminary results are encouraging. The refractive index profile images obtained during the osmosis experiment clearly show the formation of a membrane mediated boundary layer, and the volumetric flow sensors accurately measured the associated mass flow kinetics. During development, a series of leaks in the MTA fluid chambers were experienced, requiring redesign of the sealing interfaces. To date the redesigned seals have functioned without leaking.

Lockheed Martin Internal Research and Development (IRAD) funding has been used in several key aspects of the instrument development. The volumetric flow sensors have been designed and developed with IRAD funds to provide a continuous (analog) measurement of the mass transport kinetics during osmosis experiments. The Microsensor Array planned for use during the second year of the MTP program has been designed, and is currently under development, also using IRAD funds. This array will measure ionic profiles and fluid characteristics when incorporated in the MTA during the second year of the program. The fabrication of a development Microsensor Array unit has been initiated through a subcontract with the Stanford Research Institute International (SRI International).

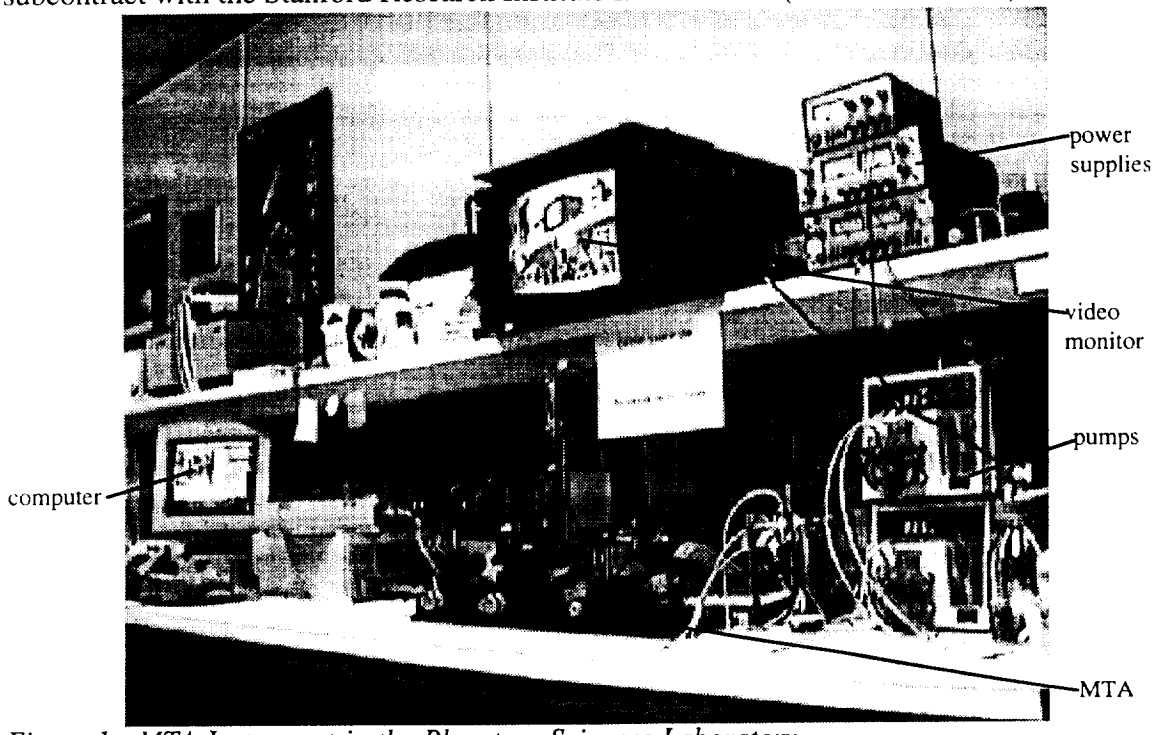

Figure 1 MTA Instrument in the Planetary Sciences Laboratory

Membrane Transport Apparatus (MTA) Instrument Overview

The Membrane Transport Apparatus (MTA) instrument is designed to perform ground based experiments involving membrane mediated transport phenomena. Figure 1 shows a photograph of the MTA instrument as it currently exists. The device is essentially a membrane that is instrumented to measure the kinetics of transport functions in terms of mass flow and fluid optical properties. The size and geometry of the MTA was developed to provide an instrument that is capable of precision measurement of these physical properties. The MTA unit is compact, modular in construction, and the fluid compartments are relatively easy to service and clean.

The MTA consists of several sub assemblies and systems to allow measurement of mass flow and fluid optical properties during experiments. The center of the instrument is the Fluids Optical Cell (FOC) assembly, which contains the experimental fluids and provides the optical and solution access interfaces. The FOC contains the Membrane Support Assembly (MSA) where the osmosis membrane is located. The FOC's are supported in a rigid frame that fastens to the optical refractometer platform and also supports the associated Volumetric Flow Sensors (developed under Lockheed Martin IRAD). The flow sensors provide kinetic mass flow data during osmosis experiments.

The optical refractometer system is mounted on an optical rail, and consists of a 3 mW red (630 nm) diode laser, beam expander, slit mask, projection screen and video camera. The refractometer functions by passing a small slit-beam of collimated laser light through the FOC prisms and experimental solutions, perpendicular to the membrane. The light that exits the MTA is displaced by an amount that is related to the refractive index of the solution. The incident slit of light covers the entire height of the fluid cells perpendicular to the membrane. The slit image is projected onto a rear-projection screen, where it is imaged using a video system that is interfaced to a frame grabber for data-image acquisition. The image produced after refraction through the fluid cells is essentially a graph of solution refractive index as a function of distance from the membrane. A reference beam is also projected onto the screen to enable calibration of the imaged profiles.

Experimental data is acquired using a software program written using LabVIEW, an instrument control package that provides a graphical user interface for control of experimental parameters. The software functions to acquire kinetic data from the volumetric flow sensors and refractometer images from the video system automatically at user defined intervals during experiments. The images and data are stored on the computer hard disk for later analysis.

A critical feature of the MTA instrument involves the characterization of fluid properties in relation to the membrane. To enable this analysis, additional software was written for processing of the stored refractometer images to allow measurement of the refractometer image dimensions, and infer physical fluid properties. This software was written in "C", and analyzes the images both in terms of dimensional scale and solution refractive index. The scale dimension measures distances in the boundary layer relative to the membrane. The refractometer axis of the image is analyzed in conjunction with the refractometer geometry to calculate an imaged offset dimension. The program outputs data for solution refractive index profile as a function of position relative to the membrane on a pixel by pixel basis over the entire refractive index profile. Each image represents a snapshot of the one dimensional fluid structure extant in the FOC at the instant in time when the image was acquired.

Fluids are manipulated in the MTA using peristaltic pumps under computer control. Algorithms for pump control software, and electrical interface circuits were developed to enable computer controlled fluid manipulations. The fluid manipulation software allows

fluids to be transferred in each FOC in several modes: (1) open loop-manual, (2) total fluid volume pumped, or (3) a closed control loop in conjunction with the volumetric flow sensors to achieve a desired setpoint.

MTA Component and Assembly Descriptions

Each of the MTA subassemblies that has been developed is described in detail in the following sections. The descriptions also include details of the development processes, and areas where difficulties were experienced in fabrication. In addition, critical components of the instrument have been identified, and design alterations for a flight instrument considered. The major sub-assemblies of the MTA include: the Fluids Optical Cells (FOC), Membrane Support Assembly (MSA), Optical Refractometer System, Fluid Manipulation System, video system, and the controlling computer. Figure 2 shows the relative locations and configurations of each of these components of the MTA.

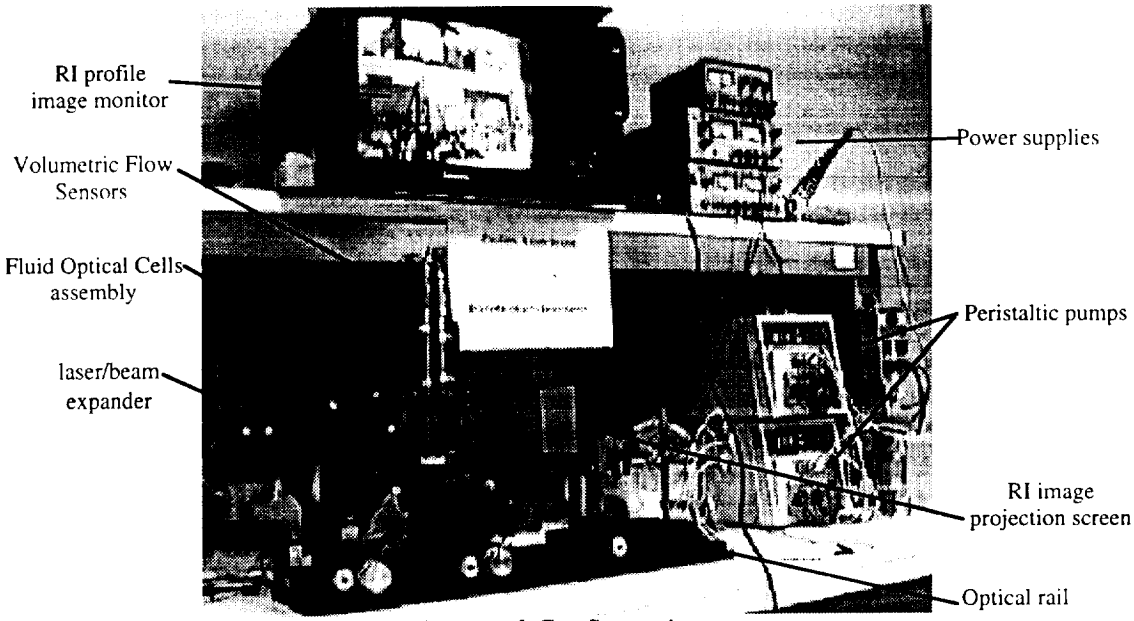

Figure 2 MTA Component Locations and Configurations

MTA Mechanical Interface

The MTA is currently set up as a laboratory based instrument. The mechanical interface is defined by three component assemblies that are fastened to an optical rail. The three assemblies include: (1)the laser mounting structure (beam expander/slit mask assembly), (2) the FOC assembly that contains the membrane and fluids under test, and (3) the projection screen for refractometer images and video camera mount. Additional equipment used in the course of experiments includes two peristaltic pumps and associated fluid reservoirs, a video monitor, several DC power supplies, sensor electrical and data interface circuits, and the controlling computer and monitor. The mechanical structure of the MTA is modular, simplifying setup and transport. The mechanical interface is rugged, and the configuration developed should be robust enough to withstand the short term microgravity (aircraft) tests planned for the second and third year of this project.

MTA Fluids Manipulation System (FMS)

A system was developed to manipulate fluids into and out of each of the two (upper and lower) Fluids Optical Cells. The system schematic for a single cell is shown in Figure 3, along with the associated data input and control output capabilities.

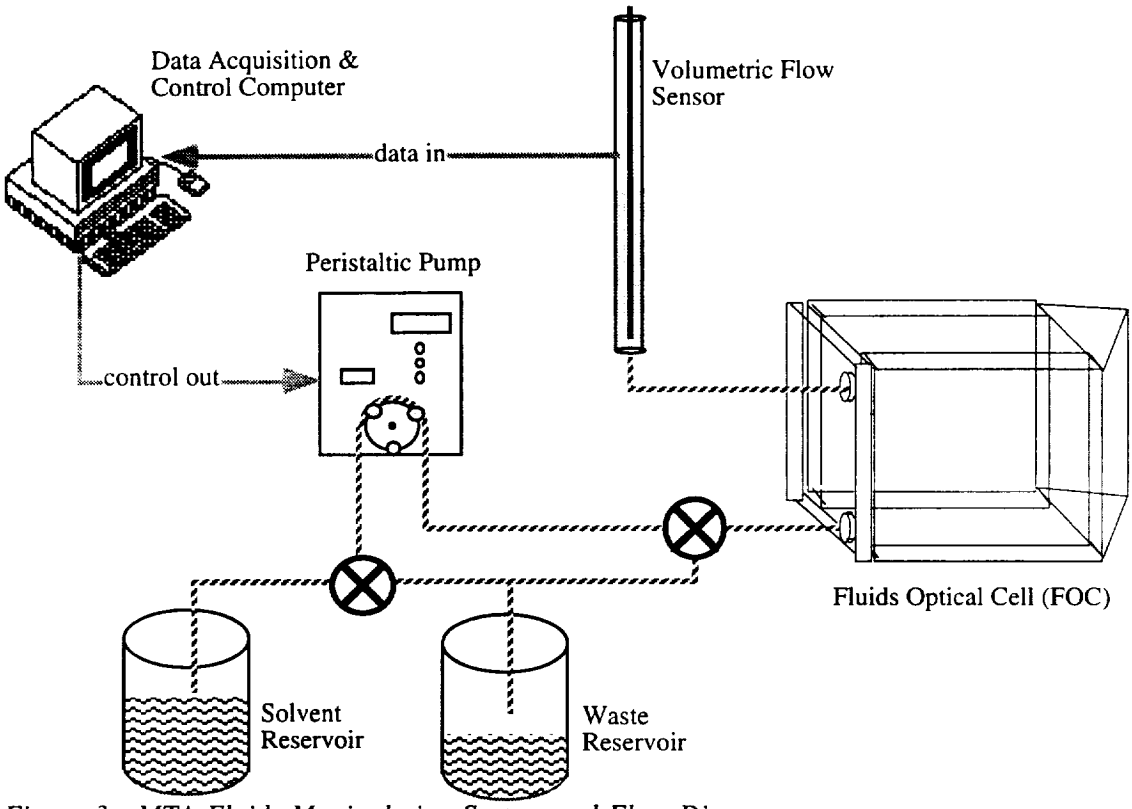

Figure 3 MTA Fluids Manipulation System and Flow Diagram

The flow diagram shows how fluids can be manipulated for each of the two FOC's. The two valves shown are manually operated, three way valves. The FMS will be upgraded in the second half of this year to use solenoid actuated valves that are under computer control. This upgraded system will then be used to control the fluid manipulations during the short term microgravity (aircraft) flights planned for the second and third year of the MTP project.

There are two peristaltic pumps, and each can move fluid in either direction, allowing both FOC filling and draining operations to be performed. The valves can be positioned to allow purging of the connecting tubing, or for filling or draining each of the fluid chambers. The solvent and waste reservoirs serve to contain the experimental fluids. The pumps are self priming, and are completely under computer control. An electrical interface was designed and fabricated to enable computer control, and software developed to enable automated fluid manipulations. The electrical interface for each pump utilizes a single 12 bit Digital to Analog Converter (DAC, 0 to +10 V) and two digital output logic lines. The analog voltage determines the pump speed, one of the digital lines controls the pump operation (start/stop), and the other digital line controls the pump direction (forward/reverse).

Each of the two pumps was calibrated using water as the pumped fluid, and an analytical balance to measure the total fluid mass pumped, over multiple time intervals. This process was repeated for a series of control voltages, and the data analyzed in terms of the mass of fluid pumped per unit time. Figure 4 shows the results of the calibration analysis for one of the pumps. The pumps are capable of using tubing of various sizes (inside diameter) to attain different maximum pumping ranges. This calibration was performed using the smallest tubing size, with a maximum pumping rate of 0.1 cc/sec.

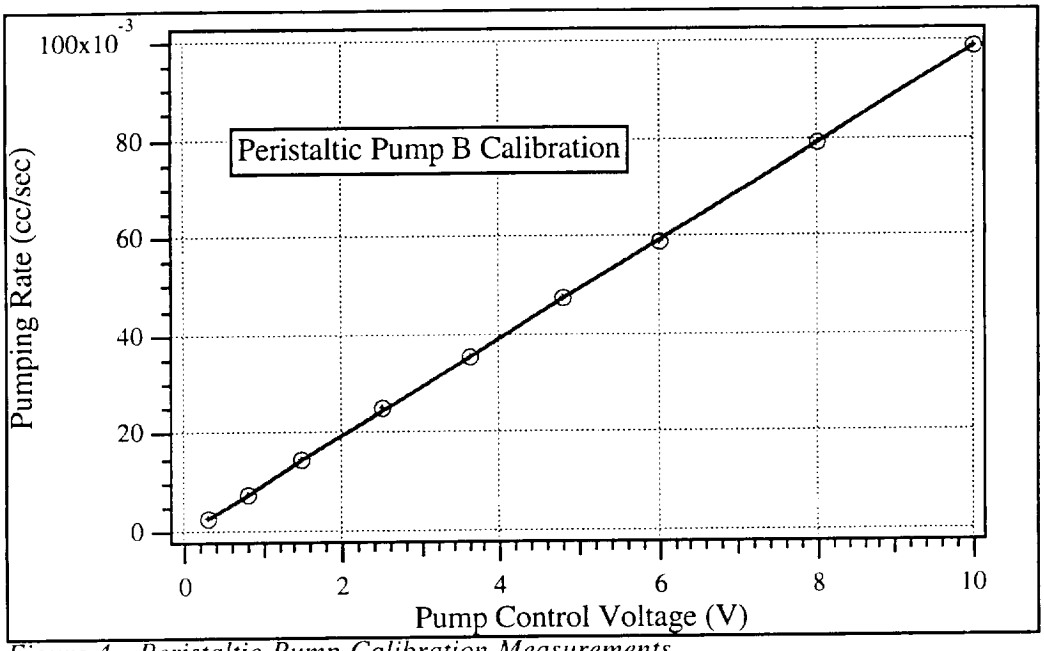

Figure 4 Peristaltic Pump Calibration Measurements

Software programs were developed to enable three different modes of fluid control. The first mode is a fully manual interface, where the user can control the pumping direction and rate of both pumps independently. Figure 5 shows the user interface screen for these manual pump control operations.

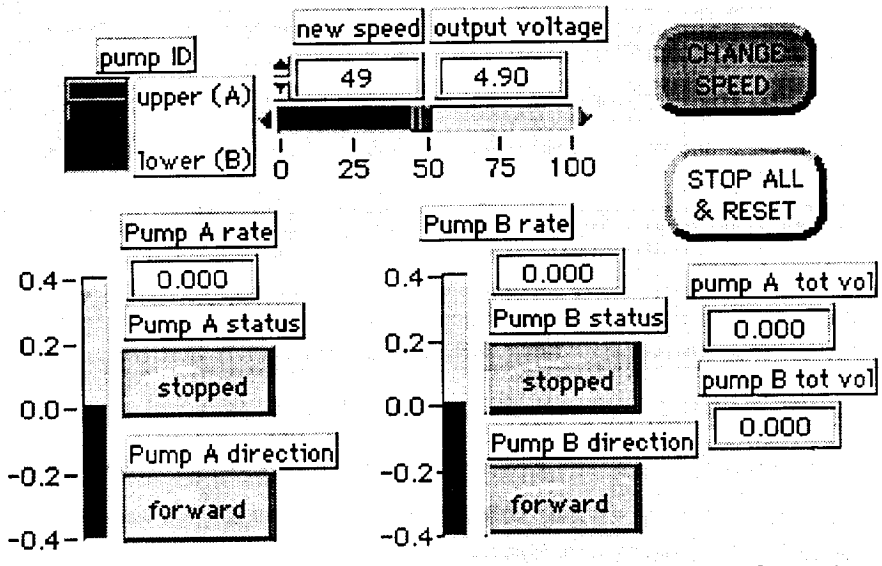

Figure 5 Peristaltic Pump Control Panel for Manual User Operations

The user can manipulate all of the controls shown in the figure using mouse and keyboard operations. The desired pump is selected at the upper left, and the desired speed is set using the upper middle control. The pumps operate by sensing the voltage signal (0 - 10 V) sent through the control interface. The magnitude of this voltage is indicated in the "output voltage" numeric display. The pumping speed for each pumps is indicated in the vertical bars (+ for filling and - for draining), and in the displays labeled "Pump A rate" and "Pump B rate". Either or both of the pumps may be addressed using the four buttons

shown at the bottom. Clicking on the "stopped" button starts the pumps, and the button changes color to indicate the pump is running. Actuation of the "forward" (fill) button changes the pumping direction to reverse (drain). The volume of pumped fluid is shown in the two displays at the lower right of the control panel. Each volume pumped is determined by the individual pump calibration coefficients that were determined as described above.

The second fluid manipulation mode is for "Total Fluid Volume" pumped. The user sets the total volume (+ for filling, - for draining), the desired pump (upper or lower), and the pump speed (cc/second). The software commands the pumps to transfer the indicated volume and terminates the operation when finished. This mode can be used directly by the user, or implemented programmatically as required in experimental sequences.

The third mode of fluid manipulation is termed "Level Fill". In this mode the computer implements a closed loop control using the volumetric flow sensor as the feedback element. The user sets the desired level in the volumetric flow sensor, the pump (upper or lower), and the pump speed (cc/second). The computer commands the indicated pump to transfer fluid until the level setpoint has been attained. The pumps will either add or remove fluid from the fluid cells, depending on the commanded setpoint.

MTA Sensors -- Volumetric Flow

The Volumetric Flow Sensor was developed using Lockheed Martin Internal Research and Development (IRAD) funding. No commercial device exists to perform this analog measurement on this scale. The sensor development consisted of a parametric analysis to determine the optimal geometry for the MTA, fabrication of prototype sensors, development and integration of interface electronics and data acquisition software, and calibration of the sensors. Figure 6 shows a schematic diagram of the Volumetric Flow Sensor.

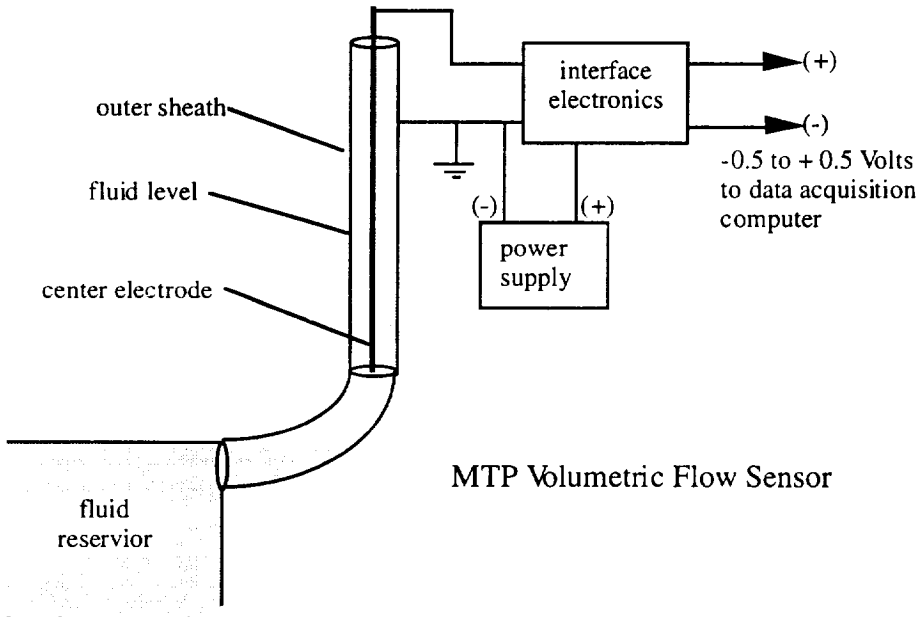

Figure 6 Volumetric Flow Sensor Schematic Diagram

The sensor geometry was optimized to have the highest sensitivity to fluid volume changes associated with solute mass transport through the membrane in the MTA. Estimates of osmotic transport rates were used to predict total mass transport in various osmosis experiments, and to develop the sensor geometry.

Figure 7 shows a parametric analysis of how the sensor sheath tube Inside Diameter (ID) and Length influence the range of operation and sensitivity of the Volumetric Flow Sensor. The sensor geometry that was chosen for the MTA was based on available materials (1/4" OD stainless steel tubing) and the predicted mass flow rates for the membrane areas in the FOC.

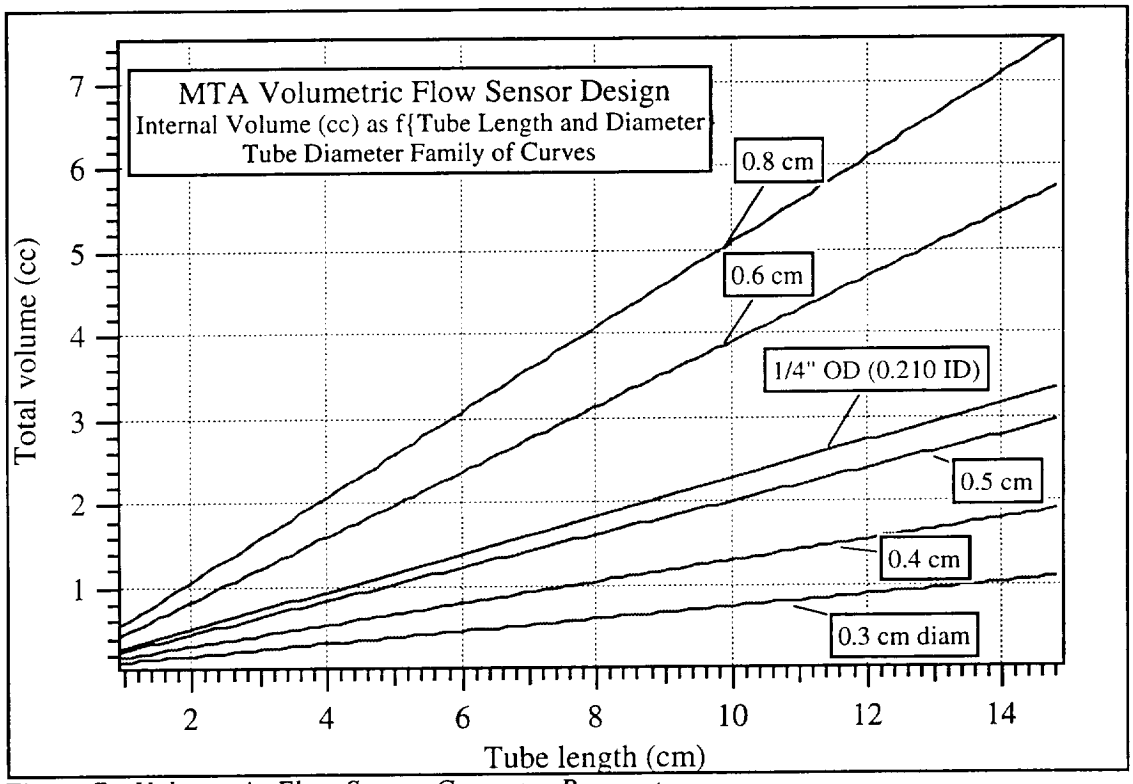

Figure 7 Volumetric Flow Sensor Geometry Parameters

The Volumetric Flow Sensor functions by measuring the fluid level within the sensor tube, and converting the measurement into an electrical voltage suitable for computer data acquisition. The sensor measurement is based on capacitive coupling between a central wire that runs coaxially down the center of the sensor tube. The sensor itself is a simple extension of a coaxial cable, with the annular dielectric insulation layer replaced with the fluid of interest. As the fluid level in the sensor changes, the associated capacitive coupling between the central wire and the outside sheath also changes. The fluid level is then directly related to the difference in dielectric constant between the measurement fluid and air (the non-fluid region).

Sensor electronics were developed to measure the sensor capacitance using a low voltage, high frequency AC signal. The high frequency alternating current is used to measure the capacitive coupling between the center electrode and the grounded outer sheath. This is necessary because there is no direct electrical contact to the fluid under measurement. The dielectric constant of the fluid materials in the sensor annular space is the measured parameter. Various trimmer potentiometer adjustments were incorporated into the interface electronic circuits to optimize the output signal for the capacitance range spanned by each Volumetric Flow Sensor. This scaling ability will be useful when subsequent generations of the MTA are fabricated and the mass flow rates and associated sensor geometries are correspondingly altered.

Two sensors were fabricated, one for each of the fluid chambers in the MTA. The sensors were calibrated using a laboratory setup that allowed small volumes of water to be measured with a mass balance, and then transferred to within the sensor body. The sensor output data was acquired, and process repeated for a series of data points. Figure 8 shows the resulting calibration plot for one of the sensors, showing that the sensor output is mostly linear with the fluid level. A polynomial fit was used for the calibration to take into account the small perturbations in the calibration curve. These perturbations are repeatable, and are presumably caused by small eccentricities in the geometry of the annular space defined by the central electrode as it passes through the sheath tube.

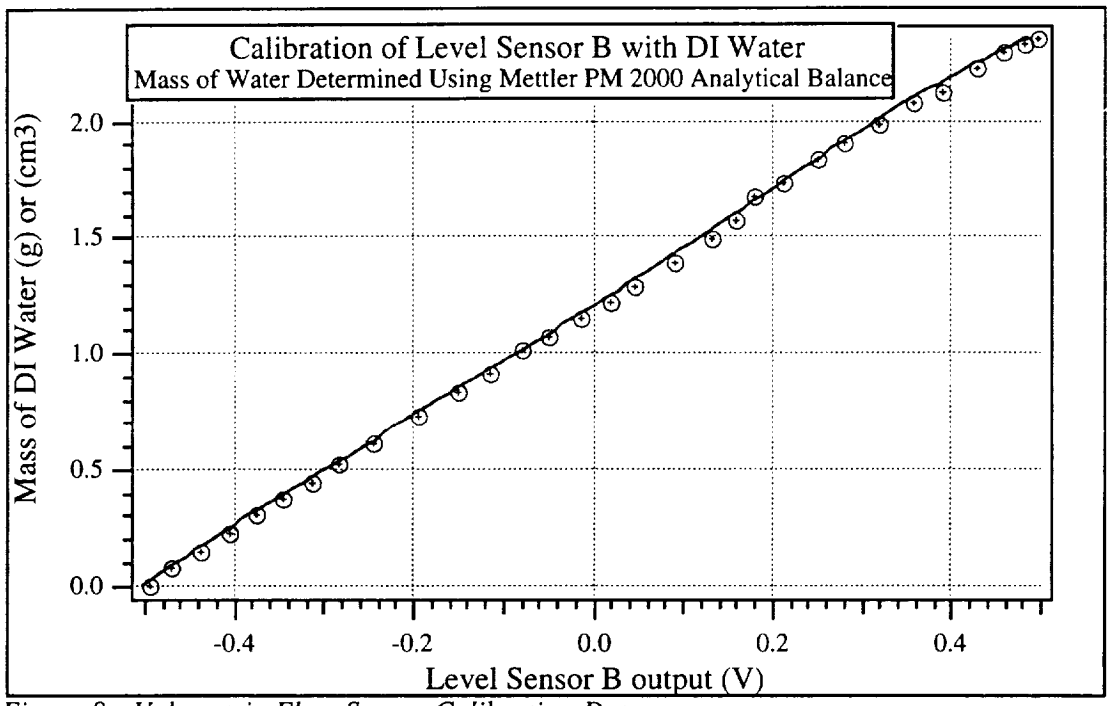

Figure 8 Volumetric Flow Sensor Calibration Data

When the initial version of the Volumetric Flow Sensors were developed and tested under static conditions, the tests showed a long term drift in the sensor signal. This drift was traced to a material used in construction of the sensor. The initial design incorporated heat shrink tubing for electrical insulation and fluid seal in the sensor electrical connection. Apparently this heat shrink tubing has some affinity for water, and water is absorbed into the tubing over the course of many hours. The absorption of water in the measurement region changes the dielectric constant of the sensor, and affects the baseline capacitance and resulting sensor output signal. This problem was difficult to diagnose because the sensor is put together using epoxy, and when assembled the sensor interior parts are not accessible. Once this problem was diagnosed, the sensors were rebuilt without heat shrink tubing, and have since shown drift free, and problem free operation.

Several overnight tests were performed on the Volumetric Flow Sensors to determine temperature effects and stability over time. The results showed a very stable sensor output, with a sensitivity of better than 90 μg fluid mass/mV output signal. The output signal showed noise at the 1 μV level. During the overnight tests, the temperature of the laboratory varied by about 5°C. This temperature change caused the sensor output to vary by less than 5 μV, indicating that the temperature coefficient is less than 1 μV/°C. These results indicate that the volumetric flow sensors are stable over a period over many hours, and essentially independent of temperature effects.

Fluids Optical Cell (FOC)

The MTA Fluids Optical Cell (FOC) assembly is the heart of the MTA instrument. These two fluid cells stack together to support the membrane, confine the experimental fluids in a one dimensional flow geometry, and provide the optical interface to required to measure solution refractive index profiles.

The FOC designed for this initial year effort is much larger than necessary for a flight instrument. The first year FOC is intended as a development unit, used to elucidate the MTA design drivers, allow visualization and optimization of the optical components of the refractometer, and to develop appropriate mechanical configurations and interfaces. Smaller versions of the FOC are planned for subsequent years in the MTP project. The next generation units will incorporate design criteria determined using microgravity (aircraft) filling experiments. A smaller FOC assembly will also simplify construction, and enable MTA experiments to be performed using appropriate quantities of physiologically and biochemically appropriate fluids. The experiments planned for this initial year of this project use standard inexpensive laboratory reagents, where total quantities are not critical.

FOC Design Considerations

The shape of the fluid containment cells dictates the geometry of the contained fluids, the associated mass transport physics, and optical interface. An analysis was performed to determine the factors that drive the geometrical requirements of the fluid cells. The fluid cell volume must be large enough to allow osmosis to occur without significant dilution of the chemical potential due to solution mixing. The fluid height on each side of the membrane must also be large enough to allow unimpeded development of stratified boundary layers, and have a constant cross sectional area so the transport processes can be modeled using one dimensional geometry. Parametric analysis of preliminary membrane experiments was performed to determine the shape factor associated with various fluid volumes. Figure 9 shows the parametric FOC design curves, and the chosen FOC geometry.

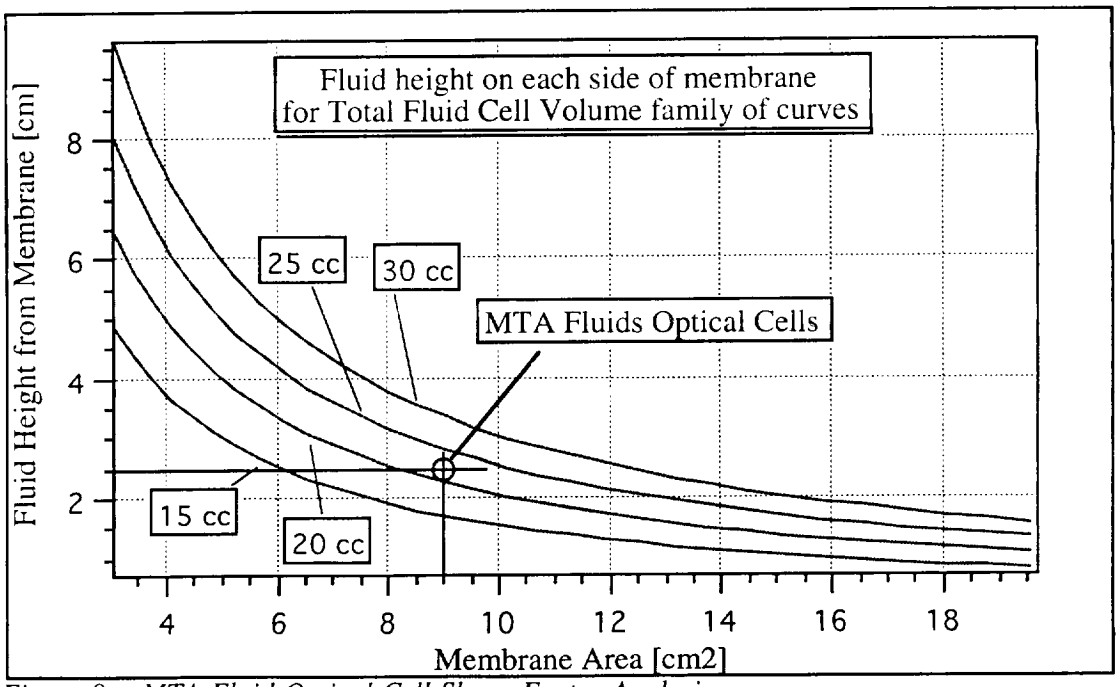

Figure 9 MTA Fluid Optical Cell Shape Factor Analysis

The FOC design is based on commercially available 47 mm diameter membranes, with the fluid compartment dimensions corresponding to the square inscribed within this diameter. The membrane area exposed to the fluids is about 9 square cm, with about 2.5 cm of fluid height on each side of the membrane. The total volume of each fluid cell is about 25 cc, including the fluid in the volumetric flow sensors. This design allows a large transport area to be active during osmosis experiments, and visualization of the light paths in the optical systems. Subsequent versions of the fluid compartments will be miniaturized to support the desired one dimensional transport geometry and minimize the fluid volume requirements.

Each of the two FOC's in the MTA has a refractometer prism, two optical windows, a pump interface plate, and an end plate. The refractometer face of the cell is a 90° (right angle) prism that is bonded at the edges to the two parallel optical windows. The optical portions of the cells are made of BK-7 glass, and have anti-reflective coatings on the optical surfaces. These glass components are bonded together with epoxy to provide a rigid, leak tight structure. A schematic diagram of the current MTA design is shown in Figure 10.

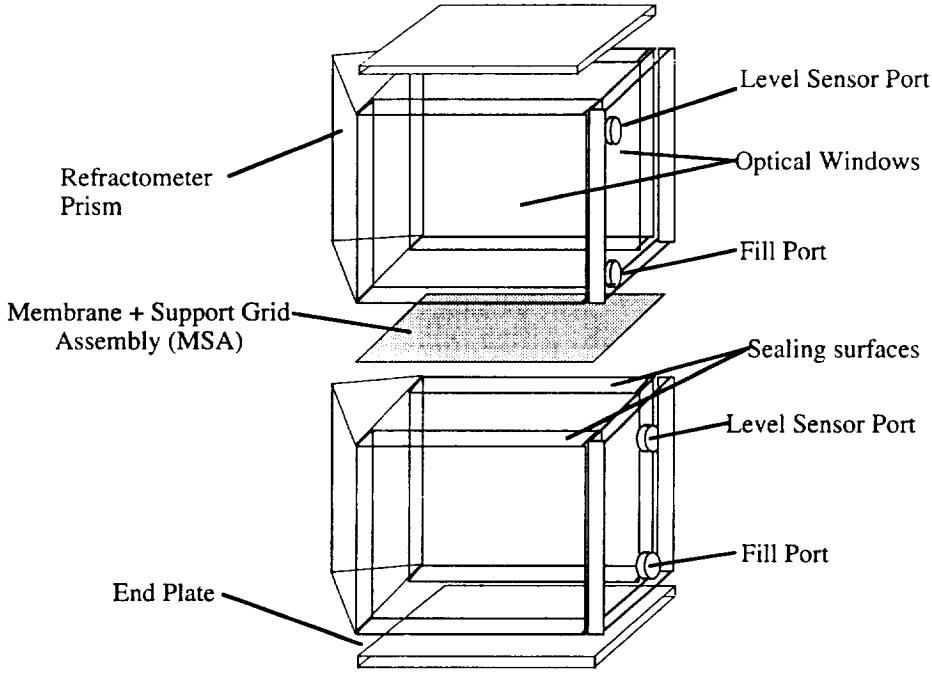

Figure 10 MTA Schematic Diagram Showing the Fluids Optical Cells (FOC) and Membrane Support Assembly (MSA).

The sealing surfaces that interface with the Membrane Support Assembly and MTA end plates were polished to a smooth finish. When assembled, the alignment of the two cells is critical, defining the relative optical geometry between the two cells and contained fluids. Each time the FOC's are assembled the relative geometry is slightly different. For this reason the optical refractometer must be re-calibrated each time the FOC assembly is disassembled/reassembled. Figure 11 shows the disassembled FOC's and one of the Kapton membrane support grids.

There are two configurations for measurement of optical parameters in the MTA: (1) optical transmission (or absorbance) though the two parallel optical windows, and (2) optical refractometer measurement of the solution refractive index profiles as a function of distance

from the membrane. The transmission configuration images the fluid directly, and is useful when colligative solute or solution molecules are optically active and visible to the video camera. The refractometer configuration images a slit of collimated laser light that passes through a prism and experimental fluids. All of the development effort to date has been related to the optical refractometer configuration; the transmission configuration has not yet been explored.

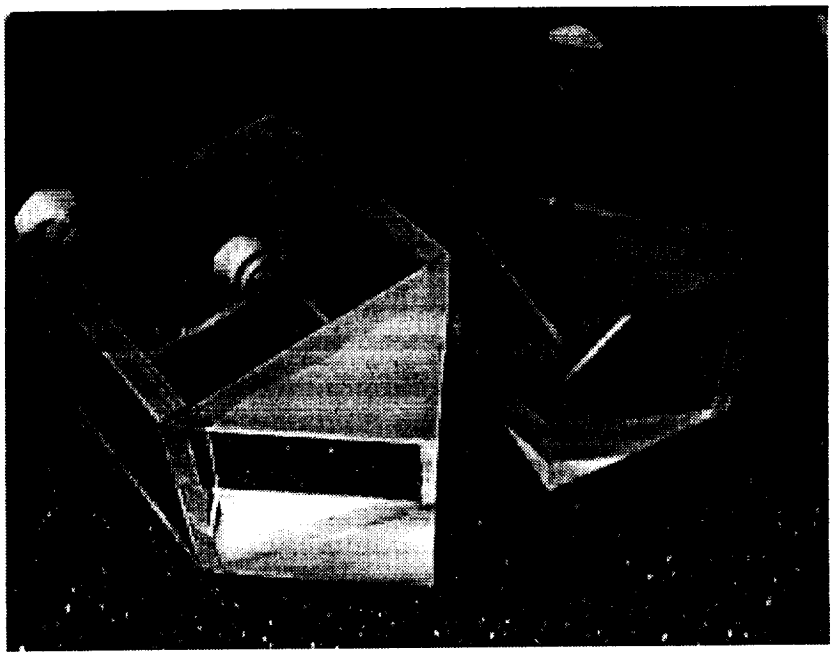

Figure 11 Disassembled MTA Fluids Optical Cells (FOC)

The FOC's stack on top of one another with the membrane and support grid assembly sandwiched in between. This assembly is held together in a support frame that provides the compressive force to effect the fluid seals and hold the assembly in a rigid optical geometry. Figure 12 shows the assembled FOC's within the support frame, together with the volumetric flow sensors.

Several fluid leaks were experienced over the course of MTA development. These ranged from very small fluid flows to major leaks that completely emptied the chamber(s). Leaks occurred in each of the cells at various corners and interfaces, requiring disassembly, repair, and rebuild. Modifications were made in each rebuild cycle, and included testing of different gasket materials and layer sequences, and repair of the sealing interfaces with silicone rubber and epoxy patches.

Membrane Support Assembly (MSA)

The Membrane Support Assembly (MSA) is a critical portion of the MTA instrument, providing the membrane to fluid interface required for osmotic mass transport to occur. The MSA is captivated between the two (upper and lower) Fluids Optical Cells, and is held together using an exterior support frame that compresses the sealing surfaces together and defines the optical geometry.

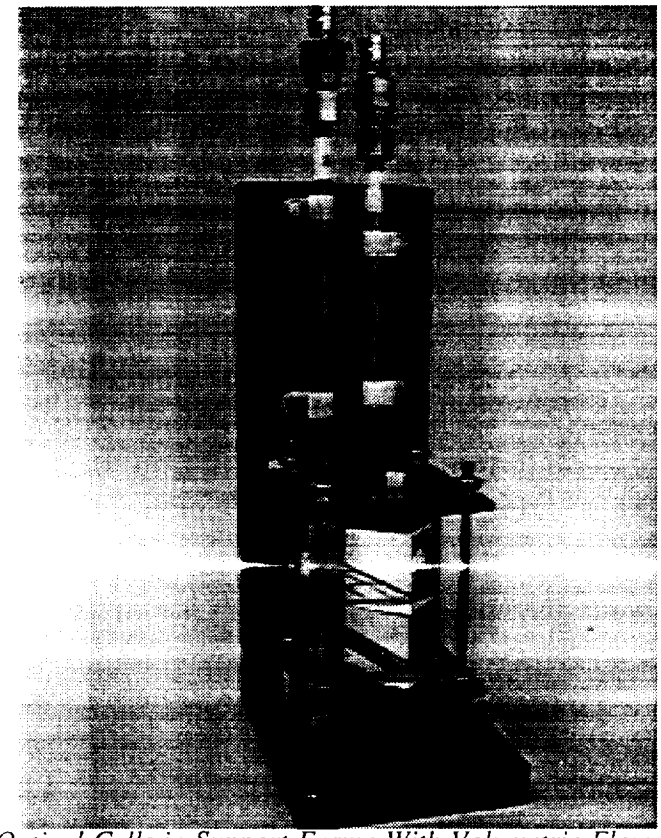

Figure 12 MTA Optical Cells in Support Frame With Volumetric Flow Sensors

As solvent molecules flow through the membrane, boundary layers may form in association with the membrane. Visualization of the formation and maturation of this boundary layer is a primary goal of the MTA instrument. Therefore, minimizing the thickness of the MSA is of primary importance to allow unhindered visualization of the fluid boundary layer as close as possible to the membrane. The latest FOC design uses thin latex rubber gaskets in the Membrane Support Assembly. The total thickness of this MSA is less than 0.5 mm, and has not leaked since completion. Viton gaskets are used to seal each end plate to the FOC end sealing surface.

The MSA design has matured through several iterations. The initial membrane support assembly used Parafilm, a wax laboratory sealant material, to provide the fluid seal at the MSA to FOC interfaces. Parafilm is very thin, bonds well to glass, Kapton, and membrane materials, and is easily removed. However, it was determined that the Parafilm did not deform well under compression, and its use resulted in numerous leaks at the MSA interface. This occurred due to the high compressive loads required on the FOC to effect the fluid seal. The high compressive load also affected the epoxy bond used to fabricate the FOC into the fluid cell geometry, and caused several major leaks and failures.

Several design iterations were required to produce an MSA design that securely captivates the membrane, and insures no leaks between fluid compartments of the fluid cell interior to exterior. The current MSA design incorporates several layers, including a semi-permeable membrane (Nucleopore, polycarbonate, 0.03 μm pore size), custom made Kapton support grids on each side of the membrane, and latex sealing gaskets. The MSA is seated within these gaskets, and sandwiched between the two MTA fluid cell halves. The entire

assembly is held together in compression by the exterior support structure, and also provides the rigid configuration for interface to the refractometer optical system.

One detrimental effect seen from the relatively large MTA size is the allowance of some physical movement of the membrane under the influence of hydrostatic pressure from the fluids on either side of the membrane. This effect has been termed "pillowing" from the appearance of the membrane under this static pressure, as it billows against the support grid. The pillowing effect is limited by the membrane support grids, and amounts to a maximum membrane displacement of about 1 mm in either direction. When this effect is integrated over the entire membrane surface, the total effect is about 0.5 cc in total volume. This volume difference can skew the measurement of volumetric flow kinetics during an osmosis experiment if the magnitude of the fluid flow is large enough to effect a change in the relative hydrostatic pressure between the two fluid compartments.

Experimental kinetic measurements performed in this configuration will be valid as long as either of two operating conditions is maintained: (1) a constant "bias" hydrostatic pressure is applied to the membrane to force the membrane into a constant geometry, or (2) the fluid level in the solute compartment is controlled to maintain zero hydrostatic pressure across the membrane. Each of these configurations will be explored for use in the upcoming series of osmosis experiments.

This pillowing effect will be less of a factor in subsequent, smaller versions of the FOC, where unsupported spans of membrane will be of smaller dimensions. It is interesting to note that this pillowing effect will not be a problem in a microgravity environment, where no hydrostatic pressure exists.

MTA Video system

A miniature video camera and frame grabber system was procured using Lockheed Martin Capital Equipment funding. The video system was integrated with the controlling computer, and capabilities developed for automated image acquisition and storage during experiments. The video system was also used to acquire the images of the MTA instrument used in this report.

MTA Optical Refractometer

The optical refractometer system is designed to measure fluid optical properties in the MTA relative to the plane of the membrane. Designs of the refractometer and associated optical mounts were iterated to optimize the performance in terms of measuring the refractive index of the fluids contained within the FOC. An analytical model of the optics was developed to allow optimization of geometrical factors associated with instrument operation, to determine geometrical factors for highest sensitivity, and to predict the performance characteristics. The algorithms generated during this model development are also used in analysis of refractometer images acquired during experiments. The major components of the MTA optical refractometer are shown in Figure 13.

Refractometer Design

The refractometer operates by passing the beam of collimated laser light through the FOC prisms and contained experimental fluids. The incident slit-beam of light covers the length of the stacked FOC's perpendicular to the membrane. The light that exits the FOC optics is refracted by an angle that is related to the refractive index of the fluid contained within the FOC. The exit light is projected onto a screen and imaged using the video system. The image acquired is essentially a graph of fluid refractive index as a function of distance from the membrane. A reference beam is also projected onto the imaging screen.

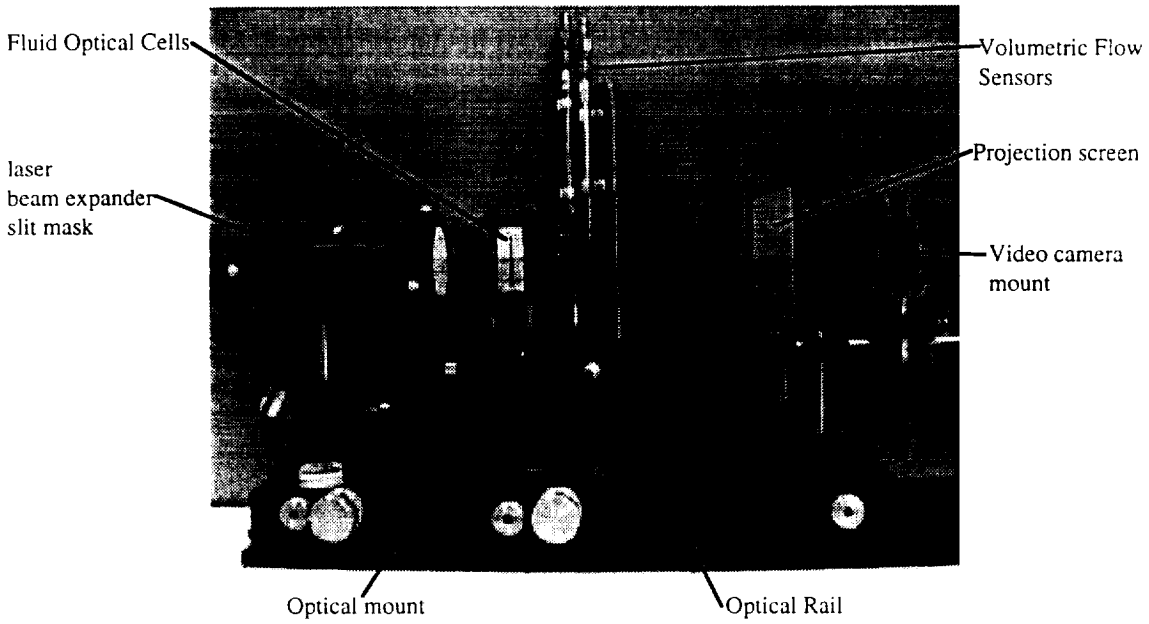

Figure 13 MTA Optical Refractometer Component Layout

The optical mount that supports the refractometer assembly allows adjustment of the FOC geometry in terms of (1) rotation angle relative to the incident laser beam, (2) translation perpendicular to the refraction beam, (3) vertical height relative to the membrane, and (4) horizontal angle (level) with respect to the gravity vector. The optical mount that performs these functions is attached to an optical rail that also supports the laser/beam expander assembly, and the projection screen and video camera. Each of these component assemblies is independently adjustable along the rail axis. The distance between the FOC and the projection screen is a critical dimension. This dimension acts as one leg of a right triangle that determines the magnitude of the refracted slit-beam on exit from the FOC.

A 3 mW red (630 nm) diode laser is the refractometer light source, and is mounted to a beam expander in a retaining fixture that insures no extraneous laser light is emitted. The laser mounting structure was designed to comply with Lockheed Martin safety regulations for operation of laser equipment (i.e. the instrument is safe for operation in a laboratory environment with no additional protection required). The beam expander has been configured to collimate the laser light, and expand the incident beam to about 5 cm diameter. A custom designed slit mask is mounted to the output of the beam expander, and masks out all but the refraction slit-beam of light that is incident upon the FOC, and a calibration figure for use in analysis of the resulting refractometer images. The reference and refraction slit-beams are both projected onto a rear-projection (frosted glass) screen, where they are imaged using the video system. The video signal is interfaced to a computer controlled frame-grabber board for data-image acquisition. The laser is also under computer control. Figure 14 shows a schematic of the refractometer components, the optical interfaces, and the angles and dimensions associated with the refractometer geometrical configuration.

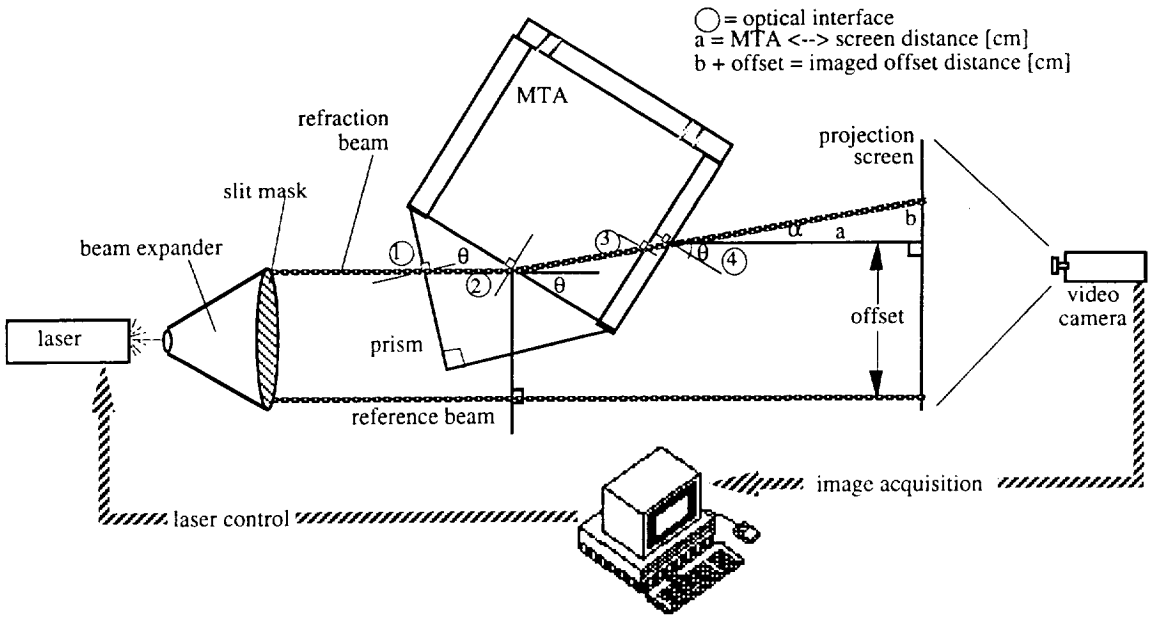

Figure 14 MTA Optical Refractometer Schematic Diagram

An analytical model of the refractometer optics was generated to optimize the configuration and enable the calculation of refractive index from the imaged profiles. The model is based on Snell's Law of Refraction, geometrical and trigonometric relations, and known material refractive indices. The model includes terms for each of the four optical interfaces encountered by the beam of laser light as it passes through the refractometer.

Two main variables are incorporated into the refractometer analytical model: (1) the FOC rotation angle with respect to the incident laser beam, and (2) the distance labeled "a" in Figure 14. The rotation angle is adjusted by manipulation of the rotary platform that the FOC's are mounted on. Rotation of the FOC assembly alters the relative incident and exit angles of the refraction beam. The distance "a" can be adjusted by physically moving the projection screen along the optical rail, closer to or farther from the FOC assembly. This dimension represents one leg of a right triangle formed by the refracted beam when projected onto the projection screen. The refraction angle α is a function of the fluid refractive index (within the FOC), and influences the magnitude of the imaged offset distance "b". The geometrical model of the MTA Optical Refractometer was used to predict the refraction angle (alpha) as a function of solution refractive index for a series of MTA rotation angles. These relations were then coupled to the beam projection geometry to produce an end to end prediction of how the refractometer performs in a variety of configurations.

Figure 15 shows the refractometer performance predicted by the analytical model for two projection distances and an assumed offset distance. The FOC rotation angle is plotted on the vertical axis, the imaged offset distance on the horizontal axis, and the contours show the solution index of refraction. The two contour plots show the magnification effect obtained by increasing the projection distance. The larger the projection distance (leg "a" of the right triangle), the larger the imaged offset distance (leg "b") for a constant rotation angle. When used in conjunction with the rotation angle, the projection distance can be used to set the full scale range of the imaged refractive index profile within the limits of the optical rail length.

Refractometer Projection Distance

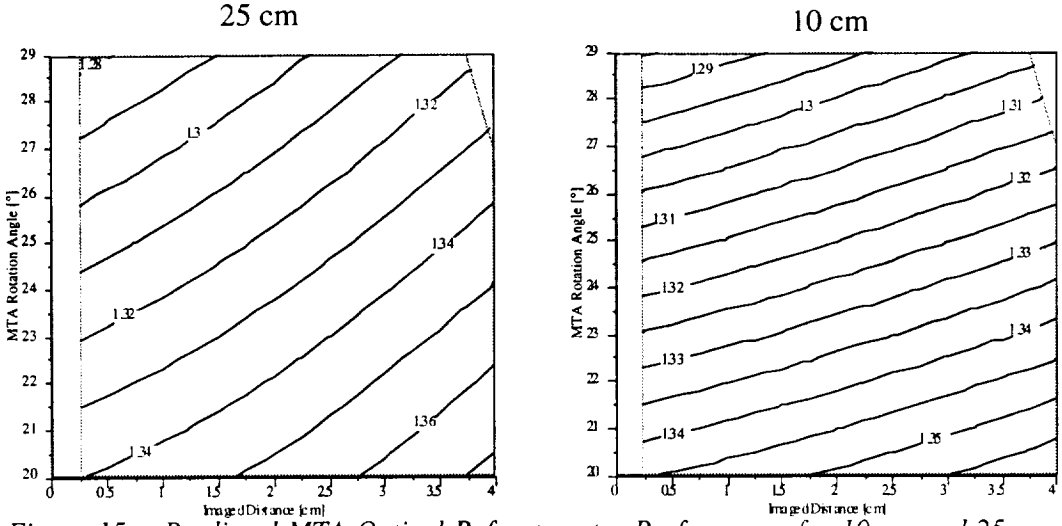

Figure 15 Predicted MTA Optical Refractometer Performance for 10 cm and 25 cm Projection Distances.

Refractometer calibration

A series of refractometer calibration experiments were performed in MTA using layered sucrose solutions of known refractive index, carefully pumped into both the upper and lower fluid chambers of the MTA. Initially the refractometer did not show optimal sensitivity, and portions of the system were redesigned to include the adjustments shown in the geometrical diagram of Figure 14. In these experiments, the lower chamber was not filled completely to prevent osmotic mass transport from occurring, acting to mix the sucrose layers. The refractometer produces an image on the projection screen that is essentially a graph of the solution refractive index as a function of distance from the membrane. An image from the calibration experiment is shown in Figure 16.

The full RGB color image is shown on the left in Figure 16, and the resulting 8 bit greyscale image extracted from the color image red plane is shown on the right. The images show the calibration figure (reference beam) on the left side, with the arrow indicating the direction of the gravity vector. The lines in the calibration grid are spaced at 2 mm intervals, with the longest line in the center representing the plane of the membrane. The vertical line in the calibration figure defines the baseline for the measurement of the imaged offset dimension, and associated fluid index of refractive. The two curved traces shown to the right of the reference figure is the refraction beam that has been refracted by the sucrose fluid layers in each of the fluid cells.

The Fluid Manipulation System was used to develop a protocol for layering the solutes into the fluid chambers with minimal mixing and optical disruption of the layer interfaces. Pure water and sucrose solutions of three different concentrations were used in both upper and lower fluid compartments in this experiment, approximately 6 ml of each solution in each layer. The relative refractive index of each layer is indicated by the position of the refraction beam in the image, with refractive index increasing to the right. The gravity vector is down in the figure, and the highest density solutions (also highest refractive index) are at the bottom of each fluid cell. This image was taken with the FOC rotated at 28° relative to the laser, and a distance of 16 cm between the FOC optical assembly and the projection screen. The solution RI's in order from the bottom are: 1.352 (382 mM sucrose), 1.345 (251 mM), 1.336 (72 mM), and 1.333 (pure water).

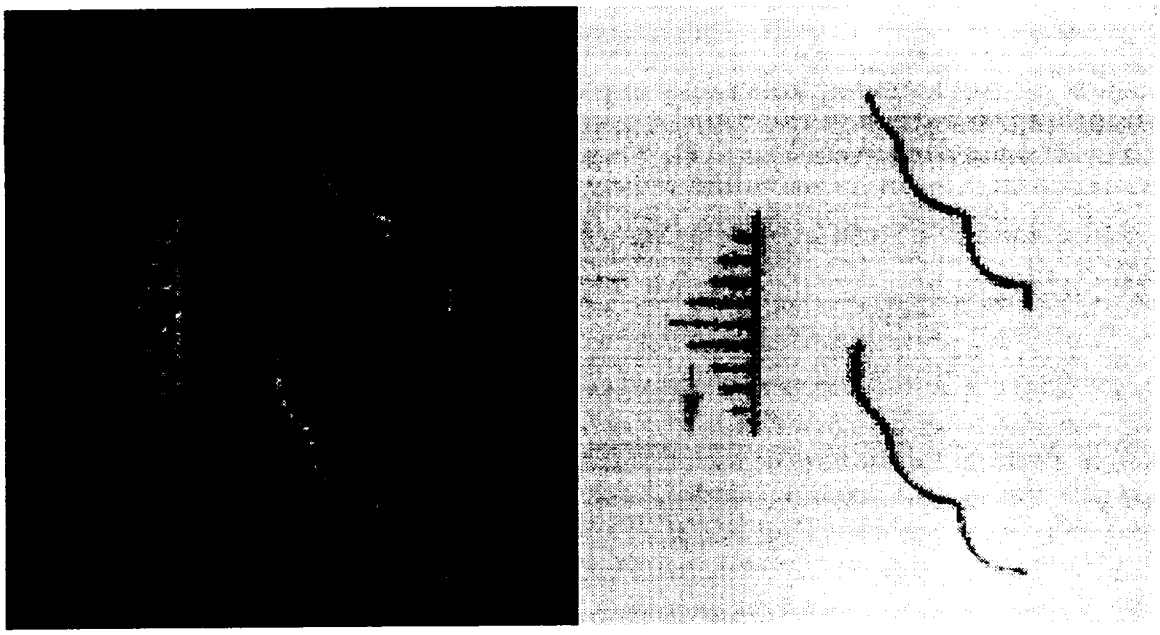

Figure 16 Image from Sucrose Layers During Calibration Experiment.
Left: RGB color image, Right: 8 bit greyscale image from extracted red plane

The calibration experiments represent an iterative learning process to find the optimal solution layer size, solute concentration, and refractometer settings. Several factors are involved in optimizing the calibration process and each of these variables. Thinner layers mix easier and are more difficult specify with the associated refractive index, but a greater number of layers can be used in the calibration. A large difference in the fluid layer density (concentration) makes the fluid interface more stable, but also represents a large difference in refractive index. Thicker fluid layers allow the unperturbed (known) solution refractive index easier to locate for calibration, but fill up the dimensional space in the fluid chamber. This consideration is illustrated in the sucrose image of Figure 16 by the fact that not all four layers are shown in both fluid compartments. The incident refraction laser slit-beam spans about 2.3 cm from the membrane in each direction, cutting off the highest layer (water) in the upper fluid cell, and the lowest layer (highest density) in the lower cell.

The optimal calibration scenario developed uses three solution layers (one pure water and two solute layers) that span the fluid concentrations of interest. This is sufficient to characterize the refractometer performance for experiments that span this refractive image range determined by the solutions.

The images obtained in the sucrose calibrations were analyzed to resolve the relations between solution refractive index and the user defined geometry's in the refractometer. Analysis of the data showed reasonably linear relations between the geometrical factors and imaged refractive index profiles, but fluid edge effects were present that distorted the relations between the various parameters. It was determined that a additional level of control was required in the optical stage to allow translation of the refraction beam to the location in the FOC where edge effects were minimized. The addition of another variable to the geometry complicates the image analysis, but removes the troublesome edge effects.

For a given series of solute layers within the MTA, changing the refractometer geometry settings even slightly alters both the absolute placement (offset), and the relative spacing (slope) of the traces imaged on the screen. To fully characterize the instrument

performance, images were acquired at several rotation angles and screen spacings for analysis. The relations among these parameters are not trivial.

Refractive Index Profile -- Image Analysis
Software was written for analysis of the images acquired from the MTA Optical Refractometer. Figure 17 shows a flow diagram that lists the software modules and algorithms associated with this code.

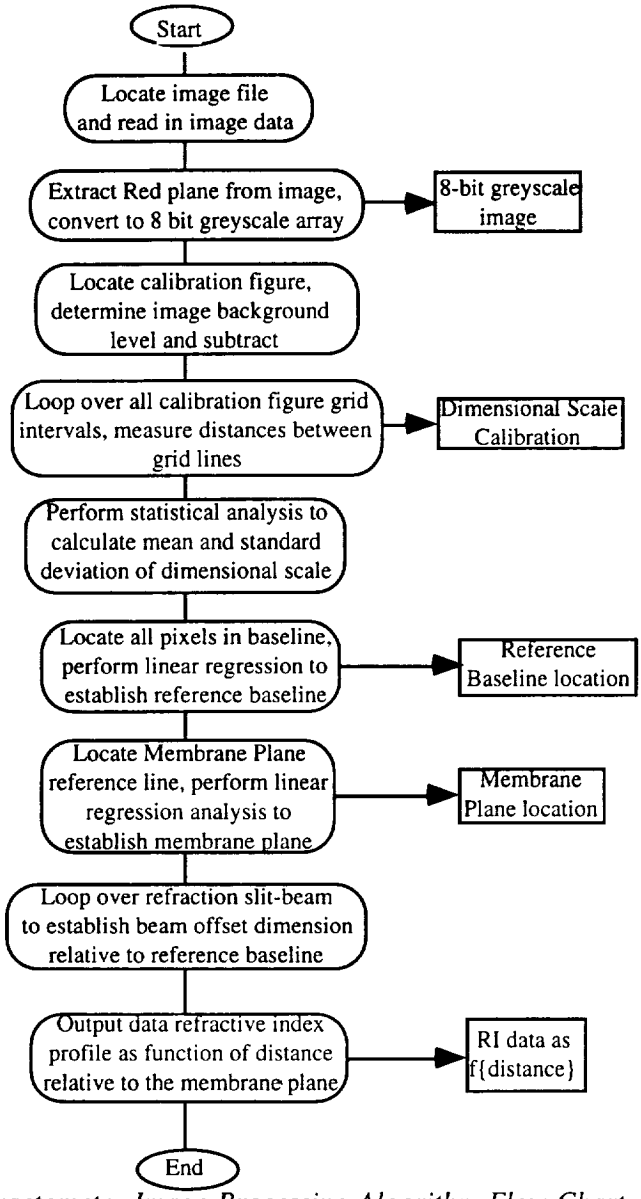

Figure 17 MTA Refractometer Image Processing Algorithm Flow Chart. Computed parameters and outputs from the program are shown in the boxes to the right.

This task turned out to be more labor intensive than anticipated, and took more time to complete than was planned. Problems were encountered with the C compiler, the image acquisition software, and the controlling computer operating system. These problems all interacted with one another to further complicate matters. However, the task is now substantially complete, and software modules now exist to process refractometer images

for calibration and experimental analysis. Further upgrades to these software modules are planned to enhance the user interface, and as upgraded versions of the compiler and image acquisition drivers become available.

The software was written in modules to simplify the analysis and enable reuse of similar functions. The software modules are sequenced to orchestrate the processing of refractometer images acquired during MTA experiments (input image data). The program first analyzes the calibration figure to scale the image dimensions, determine the relative location of the membrane within the image, establish a baseline for measurement of the beam refraction. A series of user defined threshold values are used to interpolate the position of the refractive index profile relative to the calibration baseline and the membrane. This process is performed on a pixel by pixel basis over the entire the refraction beam profile. Data is output from the program in the form of a double precision numeric array that contains distance information relative to the membrane and associated fluid refractive index imaged offset dimension for each pixel in the refracted beam image.

Figure 18 shows an example of an input image and output data points from the image processing program. Each data point in the graph represents a single pixel in the input image profile.

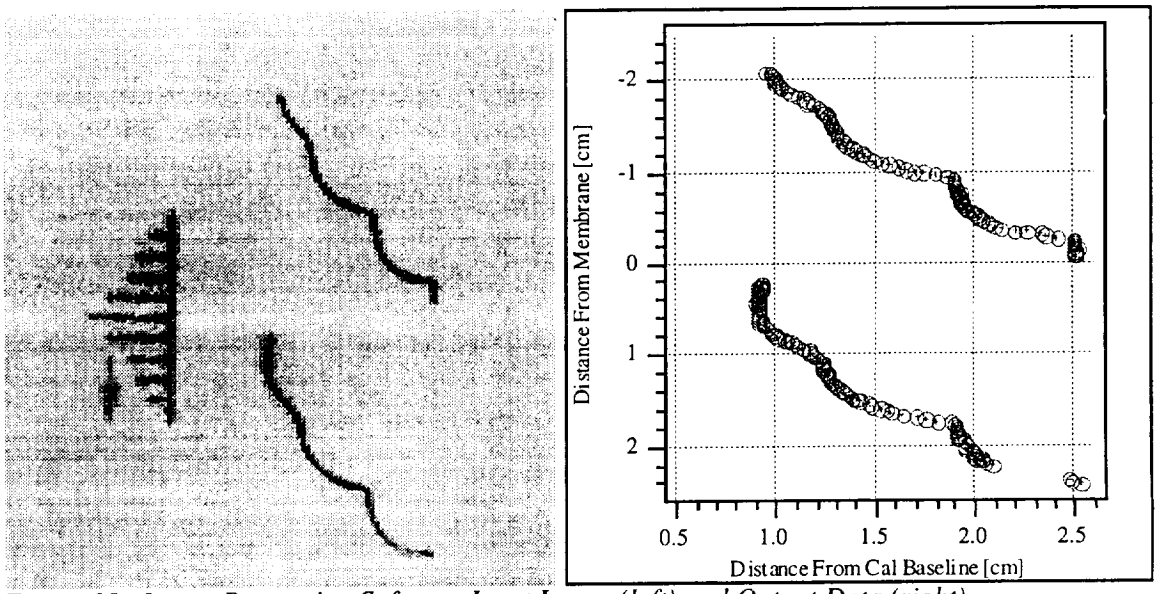

Figure 18 Image Processing Software Input Image (left) and Output Data (right)

The software is currently configured as a stand alone application that processes the refractometer images in a post-experiment batch mode. If these image processing algorithms could be incorporated into the data acquisition program, the processing could be performed on a real time basis. The current version of the instrument control program does not support the C compiler that was used to generate the code. However, an upgraded version of the instrument control software has just been released that does support this compiler. The upgrade is on order, and the image processing routines will be integrated into the instrument control package as time allows.

During the process of performing calibration experiments, analyzing refractometer images, and writing the analysis software, the FOC developed fluid leaks at various points as described in the FOC section of this report. The optical performance of the refractometer was altered each time the FOC was taken apart for repair and reassembled within the

support frame. Each repair and reassembly cycle showed changes in the relative alignment of the FOC windows and prism, alignment of the upper and lower FOC relative to each other, and the overall alignment of the FOC's within the support frame relative to the laser.

The final element of the calibration procedure is a reconciliation of the predicted optical performance with the data obtained in the calibration experiments. This task is currently in progress.

Experimental Data Acquisition and Control Software

Software was written to enable automated data acquisition during experiments. The software calculates experiment elapsed time, controls the video frame grabber board for refractometer image acquisition, and monitors various sensors throughout the instrument. The sensors monitored include ambient temperature and the volumetric flow sensor associated with each fluid compartment to measure the mass flow kinetics. The sensor data is written to a data file on the computer hard disk for post experiment analysis.

The software was written using LabVIEW, a graphical development tool for instrument control. The program consists of two separate windows, the Panel and the Diagram. The Panel window contains the user interface, complete with all input fields and output displays. The Diagram window defines the actual program structure, showing all symbolic links between the program elements. The program elements consist of input/output from the Panel window, internal processing algorithms, and processing associated with subroutines. Figure 19 shows the Diagram window for the primary module of the MTA instrument control program.

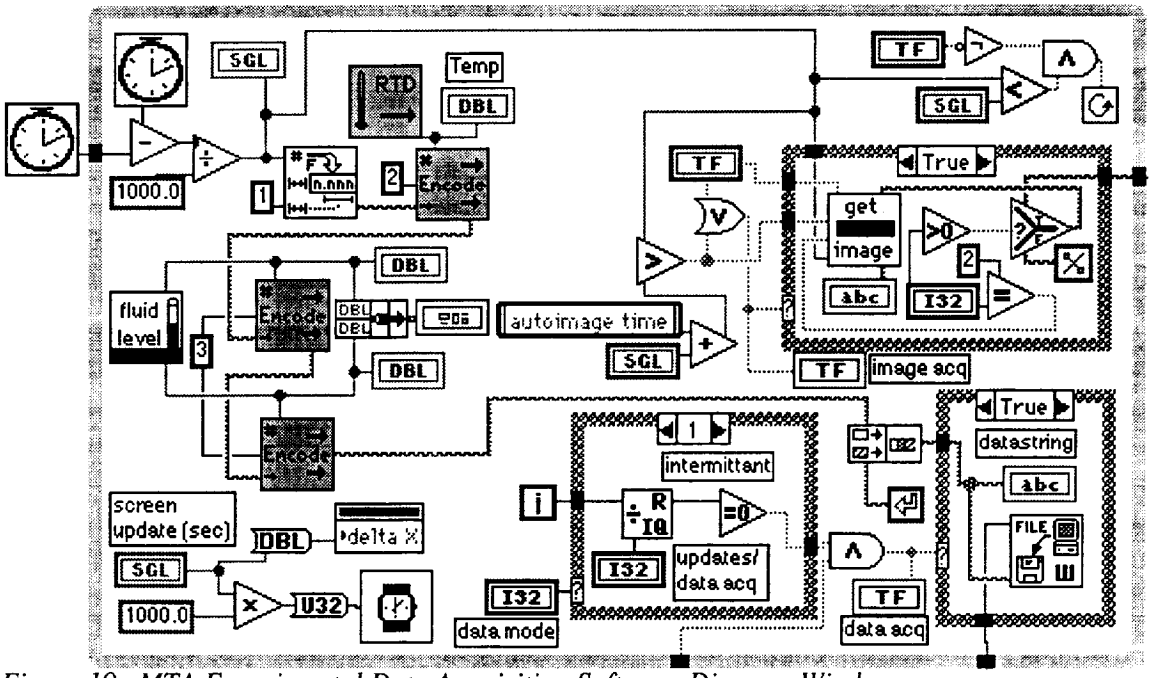

Figure 19 MTA Experimental Data Acquisition Software Diagram Window

There are no lines of code, the lines that connect the various modules define the programming. The outermost (gray) structure represents a "while" loop. This is the main of the program where the most time is spent, essentially looping through all the elements shown over and over until the experiment end time has been reached. Each of the structures shown is analogous to a subroutine that performs specific tasks, i.e. image acquisition, measurement and conversion of sensor voltages, write operations to the data

file, and so on. The square icons each represent a subroutine that has its own Panel window and associated Diagram that defines the programming. Modules are shown for controlling the data and image acquisition timing, and for communication with the front panel. The upper left portion shown in the diagram computes the experiment elapsed time, a parameter that is also used in several other parts of the program. The upper right region controls the frame grabber for refractometer image acquisition and storage (the "get image" icon). The "get image" subroutine also controls the laser that provides the incident light for the refractometer, triggers the frame grabber for acquisition of a refractometer image, and stores the image in several user selectable formats. The remainder of the program is concerned with data acquisition for display in the Panel window and for writing to the data file. The software that controls the Fluid Manipulation System as described earlier in this report was also written in LabVIEW, but is a separate program from this instrument control software shown here.

Initial MTA Osmosis Experiment

The first osmosis experiment was conducted in the MTA during March of 1996. The experiment used sucrose as the colligative solute, and was performed in both orientations with respect to the gravity vector. The experiment was performed to prove the concept of this technique for visualizing the boundary layer formation dynamics and for developing experimental protocols. Figure 20 shows the front panel display for this experiment.

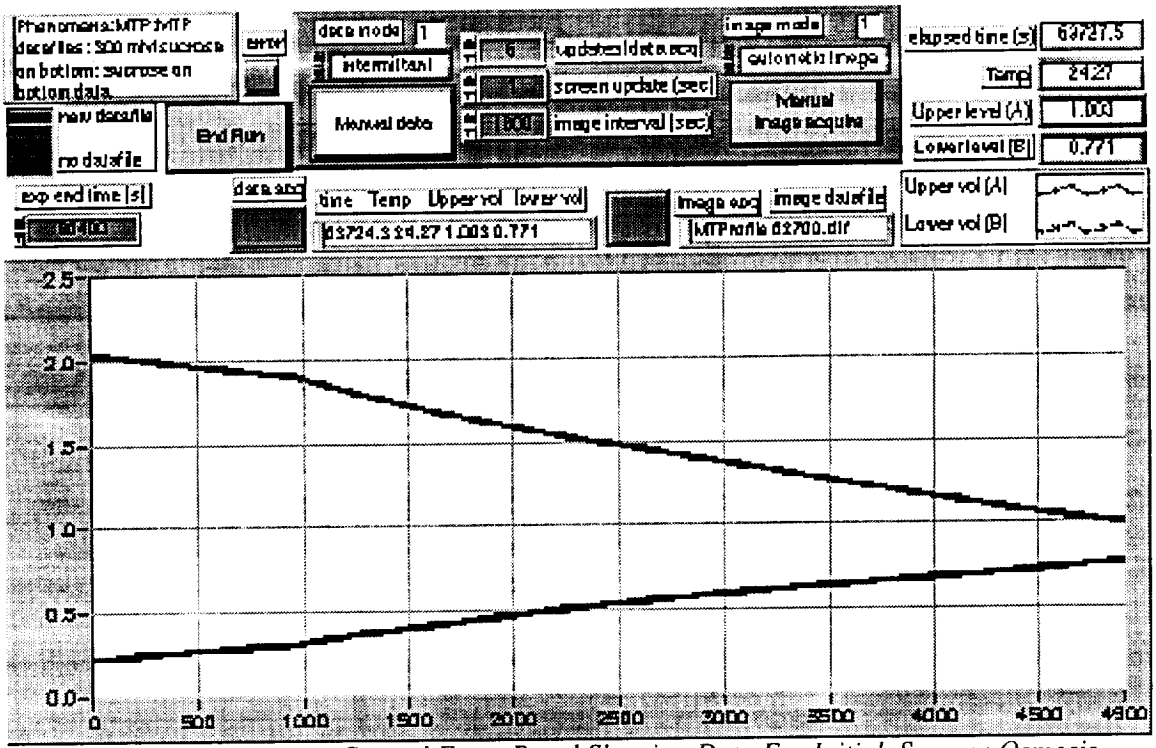

Figure 20 MTA Instrument Control Front Panel Showing Data For Initial Sucrose Osmosis Experiment

The refractometer was uncalibrated, so the experiments did not produce quantitative results. The qualitative results are encouraging, with the refractive index profile clearly showing the dynamics of membrane mediated mass transport and boundary layer formation. The volumetric flow sensors also performed well, providing kinetic data of osmotic mass transport through the membrane.

The refractometer acquired images of the refractive index profiles during these experiments. Figure 21 shows the profiles obtained for the sucrose on top orientation, where osmosis acted to transport water from the lower fluid cell to the upper cell from the bottom, creating an unstably stratified layer.

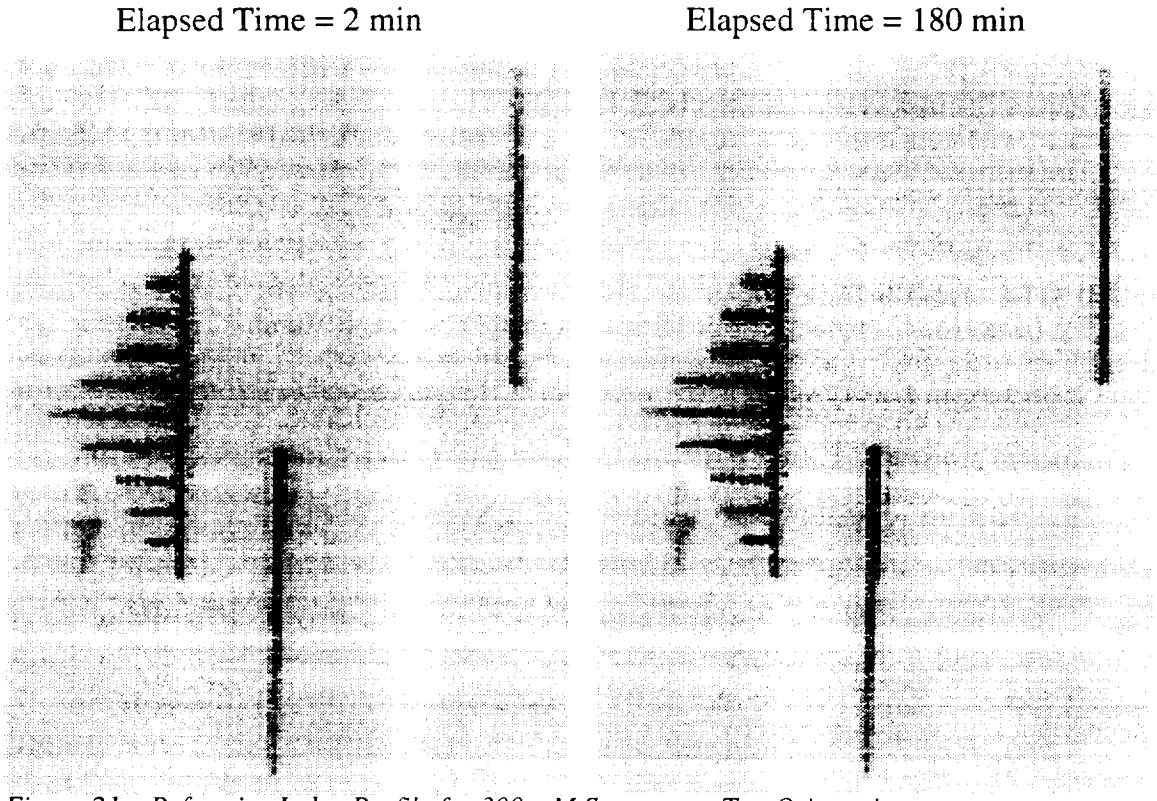

Figure 21 Refractive Index Profile for 300 mM Sucrose on Top Orientation

In this orientation with a lower density solute entering a higher density solution from the bottom, gravity acts to mix the fluids through buoyancy driven convection. The image shows higher refractive index values displaced farther to the right.

In this orientation gravity acts to continually mix the solution in the upper fluid cell, and present fresh high chemical potential solute to the membrane surface to drive the osmotic process. Schlieren was visible within the upper fluid cell as the convective mixing occurred indicating that water was transported through the membrane into the upper fluid cell. The profiles shown represent the experiment starting condition (left image), and after an elapsed time of three hours (right image). There is virtually no difference between these two profiles due to the gravity driven convective mixing.

The inverse gravity orientation was also tested, with the sucrose solution in the lower fluid cell. The graph shown on the instrument control Panel of Figure 20 shows the data for the volumetric flow sensors in each of the two fluid compartments in the inverted orientation. The sucrose solution was in the lower fluid cell in this experiment, and osmosis acted to transport water from the upper chamber (upper graph trace) to the lower chamber (lower graph trace). Figure 22 shows some of the refractive index profiles imaged during the inverted orientation experiment. The starting profile (elapsed time=0) for this experiment showed two offset vertical lines, representative of homogeneous solutions in each of the fluid chambers, essentially the inverse of the images shown in Figure 21.

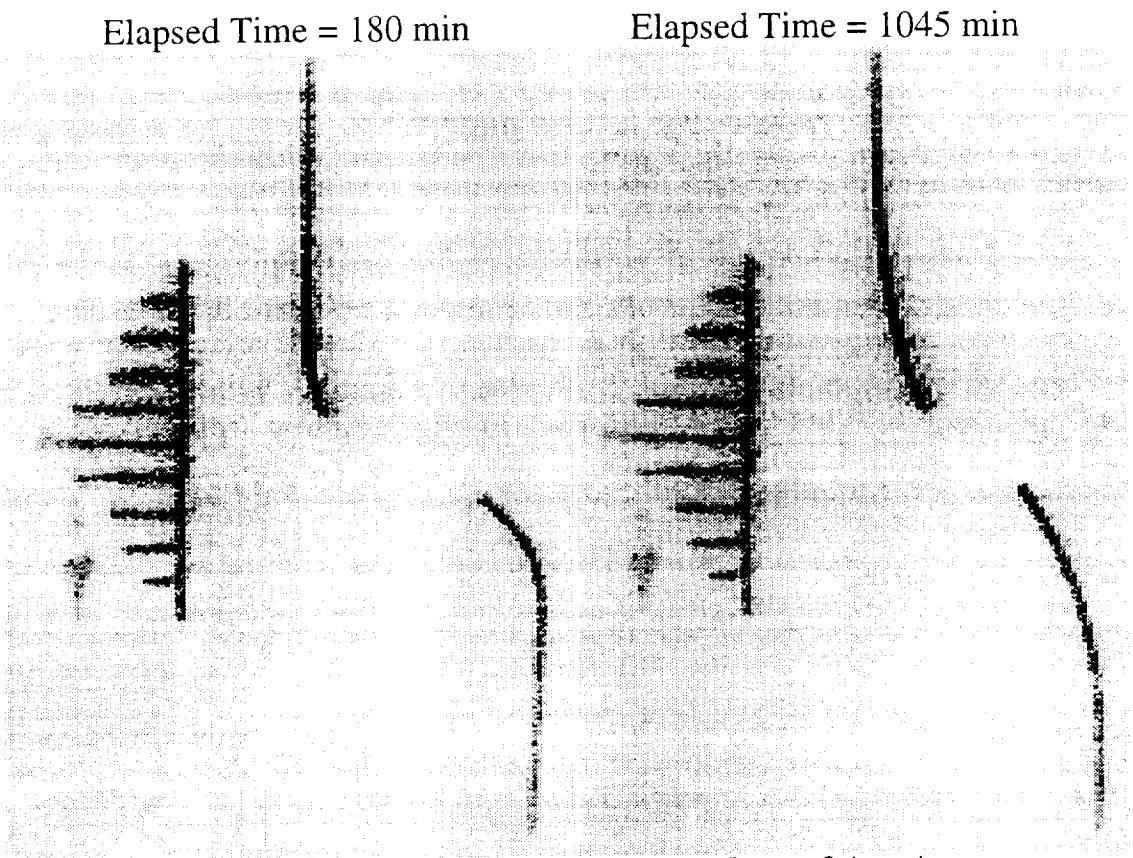

Figure 22 Refractive Index Profile for 300 mM Sucrose on Bottom Orientation

In this inverse orientation, osmosis acts to transport the less dense water through the membrane onto the more dense sucrose solution from the top. Gravity acts to enhance the formation of a stably stratified boundary layer in association with the membrane. As this boundary layer develops, the concentration of sucrose present at the membrane surface is reduced, and consequently the osmosis mass transport rate is also reduced. These refractive index profiles clearly show the boundary layer formation.

As noted before, a series of fluid leaks was experienced during the MTA development. These leaks were from a variety of causes, and included both leaks between the cells through the membrane (leaky membrane seal), and from the fluid cell interiors to the outside. The profiles shown in this inverse orientation osmosis experiment also indicate a leak between the fluid cells. The profile in the upper cell should remain straight over the entire experiment if the membrane is truly semi-permeable. The presence of the curved profile in the upper cell indicates that the colligative solute (sucrose) has diffused through the membrane into the upper cell. This type of leak in the system invalidates the experimental results because the mass transport is no longer driven purely by osmosis, but is instead a combination of hydrostatic, diffusive, and osmotic potentials. Preliminary indications are that the redesigned Membrane Support Assembly has eliminated the leak between the two fluid compartments.

Microsensor Array Developmental Unit (LMA funded)

A design was generated for the development version of the Microsensor Array. This development version is a preliminary fabrication of the array to prove the concept and work out any problems in the fabrication process. The array has four sensors of each type (cation ISE, anion ISE, temperature, and electrical conductivity) arrayed to measure the profiles in relation to the array edge. This array is scheduled for delivery to LMA this fall for testing and analysis. The final version of the array will include 8 sensors of each type, and is planned for incorporation into the MTA during the second year of the MTP project. A contract was established with Stanford Research Institute (SRI International) for fabrication of the development version of the Microsensor Array (LMA IRAD funding, February 1996). Figure 23 shows a schematic diagram of the development version of the Microsensor Array.

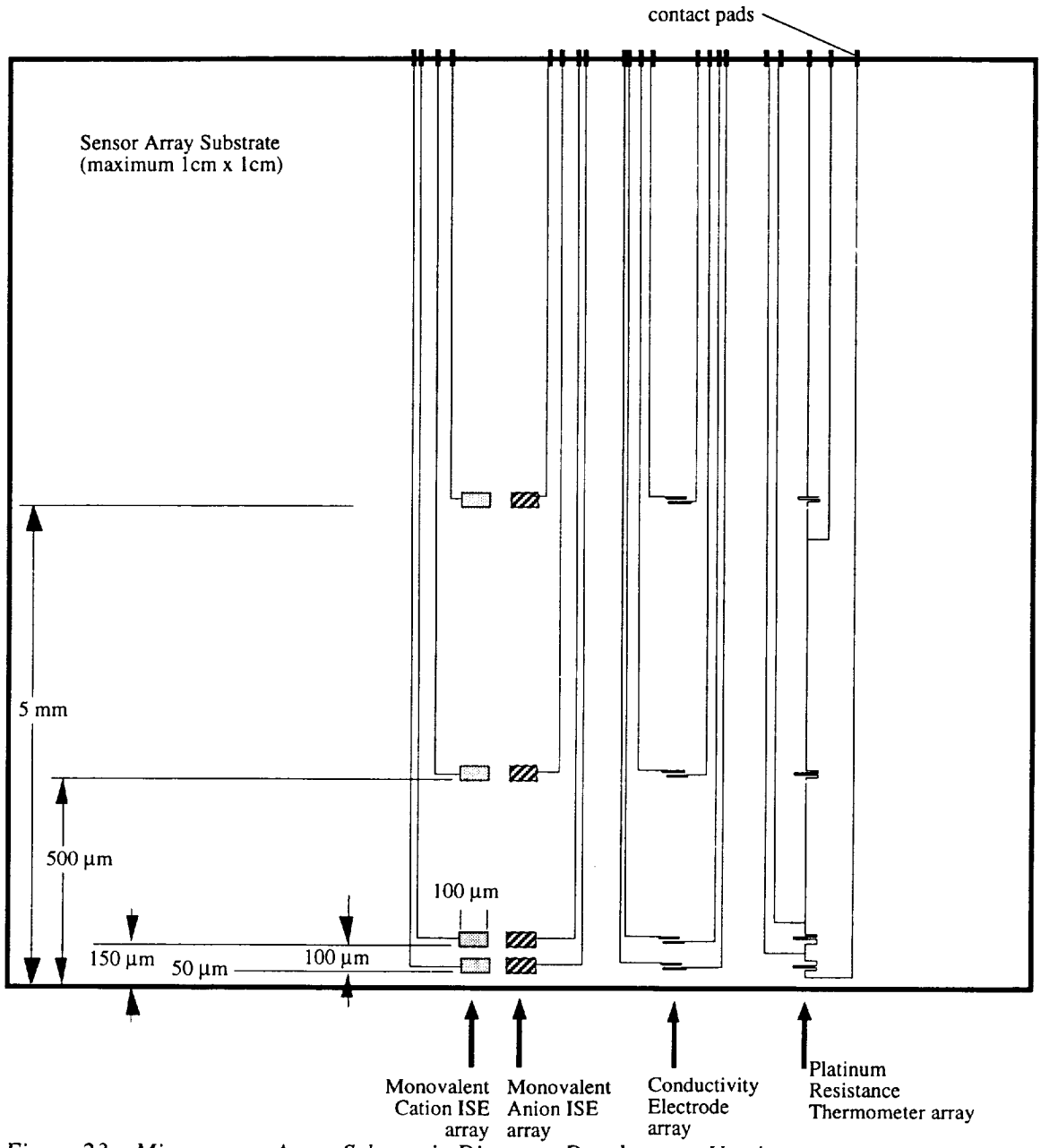

Figure 23 Microsensor Array Schematic Diagram, Development Version

Microsensor Array

Electrical and Data Acquisition Interface Definition (LMA Capital Funding)

The interface for electrical and data acquisition was defined for the Microsensor Array. The interface includes circuits specific to each of the sensor types in the array, and analog multiplex circuits to read each element in the array separately. The sensor types present in the array include: (1) high impedance voltage follower circuits to measure the electrochemical potential generated by the Ion Selective Electrodes (ISE) for measurement of cations and anions, (2) electrical conductivity measurement electronics, and (3) an electrical current source for the Platinum Resistance Temperature Detectors (Pt-RTD). These interface circuits have been designed, and are currently being fabricated on a breadboard. The breadboard will fit into a chassis that is configured to operate with the controlling computer. This work is being performed as time allows, and should be complete sometime during summer 1996. Figure 24 shows a schematic diagram of the Microsensor Array electrical and data acquisition interface.

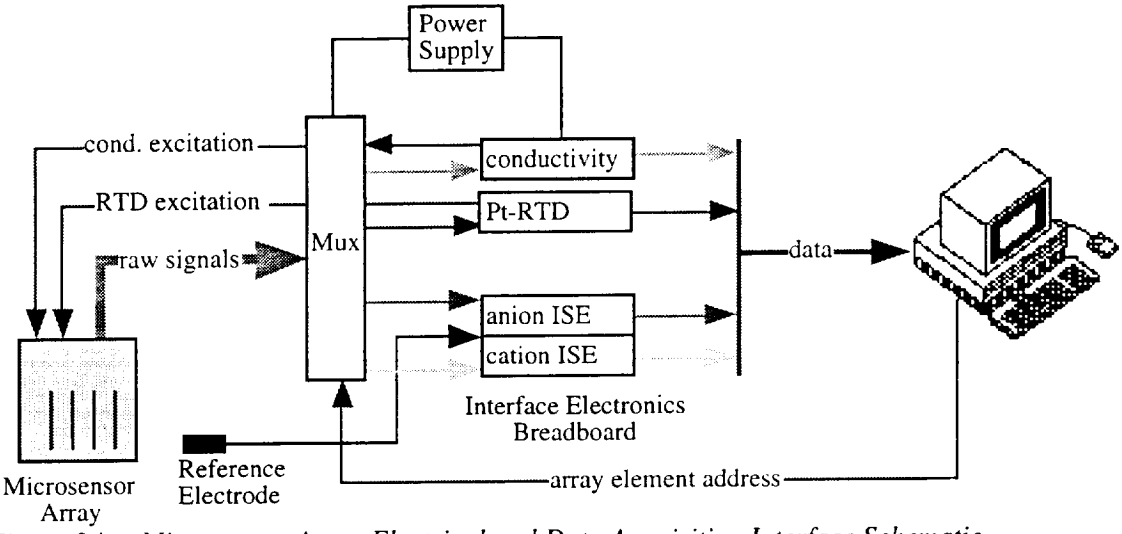

Figure 24 Microsensor Array Electrical and Data Acquisition Interface Schematic